Numerical analysis of near-field optical trapping using tapered fiber probe

Guoping Zhang*, Zhongru Zhu, Yanping Li, Ge Xia, and Qi Lin

Department of Physics, Central China Normal University, Wuhan, 430079, China

ABSTRACT

A new scheme for optical trapping is presented in this paper. The method is based on a tapered fiber probe with a tip diameter less than a light wavelength. A three-dimension gradient optical field is formed within the optical near field of the fiber probe, and a particle approaching the fiber probe tip will be trapped. The evanescent electromagnetic field in the vicinity of the fiber tip is calculated by the multiple multipole method (MMP). The intensity distributions and the trapping potential of the near fields of the tip versus the longitudinal and transverse distances from the tip are analyzed respectively. The trapping force is obtained for a dielectric particle. The numerical calculating results show the availability of this method.

Key words: optical trap, near-field optics, fiber probe, scanning near-field optical microscope

1. INTRODUCTION

Optical trapping by a single-beam gradient force trap was proposed by Ashkin *et al.* for the first time.[1] Since then, this method has been developed as an optical tweezers technology, and extensively used for manipulation of various submicron-size dielectric particles and biological structures (such as viruses, bacteria and yeast cells).[2,3] However, conventional optical tweezers, based on the gradient field near the focus of a laser beam, have a diffraction-limited trapping volume.

Scanning near-field optical microscopy (SNOM), developed recently from the combination of the scanning probe technology with the optical microscopy, offers an optical image technology with an ultra-high resolution beyond the diffraction limit.[4-6] The resolution capability of the SNOM system is determined by the transmission property of the fiber probe, such as the output photon flux density from the probe and the tip size of the probe. Nowadays its longitudinal and transversal resolutions have reached 0.1nm and 7nm respectively.

In this paper, a novel high-resolution optical trapping scheme is presented by a tapered fiber probe used for SNOM. Because the tip diameter of the fiber probe is smaller than a light wavelength, the near field close to the tip mainly consists of evanescent components which decay rapidly with distance from the tip.[7-9] Thus a three-dimension gradient optical field is formed within the optical near field of the fiber probe. When one particle approaches the fiber probe tip, it will be trapped by a three-dimension optical trap, which is produced from the action of the three-dimension optical gradient force. As this type of optical trapping appears within the optical near field of the fiber probe tip, it is called as the near-field optical trap.

* Correspondence: Email: gpzhang@phy.ccnu.edu.cn

In *Optical Sensing, Imaging, and Manipulation for Biological and Biomedical Applications*, Robert R. Alfano, Ping-Pei Ho, Arthur E. T. Chiou, Editors, Proceedings of SPIE Vol. 4082 (2000) • 0277-786X/00/$15.00

2. TAPERED FIBER PROBE

Tapered fiber probes used for the scanning near-field optical microscopy are generally fabricated by local melting and pulling single-mode optical fibers.[10,11] An about 2-meter-length single-mode fiber stripped off a short section of jacket in its middle part is heated locally by a beam of CO_2 laser, simultaneously an external pulling force is applied on two ends of the fiber. When it is broken, a tapered fiber probe is obtained. Appropriate choosing the laser intensity, the heating length and time, and the pulling force strength can be used to yield fiber probes with various tip sizes and taper shapes. The tip diameters of the fiber probes used for the SNOM system are required less than an optical wavelength, e.g., tens to hundreds of nanometers for the visible light. Figure 1 gives schematic diagrams of the conical-taper and the parabolic-taper fiber probes.

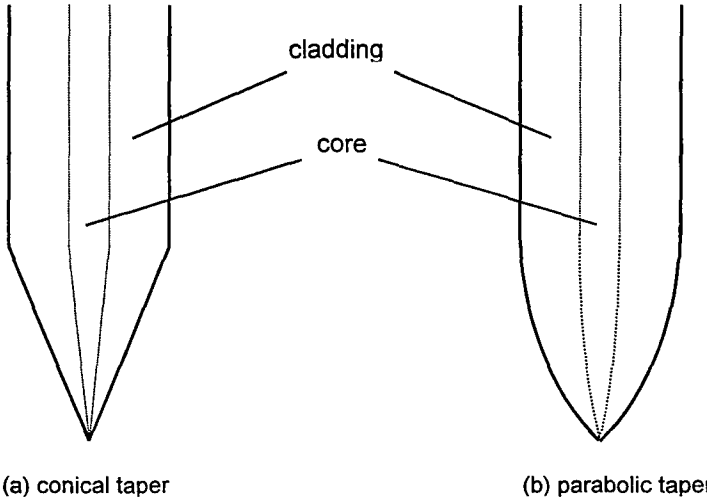

Fig.1. Schematic diagram of tapered fiber probes with (a) a conical taper and (b) a parabolic taper. The areas within the dash lines stand for the fiber core, and those between the solid lines and the dash lines for the fiber cladding.

Both the diameters of the cladding and the core of the tapered fiber probe decrease gradually along the taper, and they are usually assumed to maintain their initial ratio. The modes in the beginning of the fiber taper exhibit first the core-guided modes, and they contracts slightly. After propagating a certain distance along the taper, the core-guided modes spread into the cladding, and gradually couples to the cladding-guided modes, for which the boundary condition becomes the cladding/air boundary.

The waveguide structure of the tapered fiber is changed with a different taper shape, thus results in different transmission property. It is shown by the local modal analysis that, the mode field is first the core-guided mode and contracts slightly along the taper, then spreads into the cladding and gradually couples to the cladding-guided modes. When the tip size of the tapered fiber is less than an optical wavelength, the evanescent wave becomes the major part of the optical near field from the tapered fiber. Meanwhile, due to the tip scattering, the evanescent wave is mostly concentrated at the axial direction, and the lateral optical field decreases gradually. So optical field gradients are formed near the tip of the

tapered fiber probe.

The transmission properties and the electromagnetic field distributions are different for the conical and parabolic tapered fiber probes.[9] Generally, the parabolic tapered probe has a transmission efficiency of almost one order of magnitude higher than the conical one. The electromagnetic near-field distributions of these two probes are more focused while their taper angles increase.

3. THEORY

A laser beam is coupled into the single-mode fiber from the end opposite to the tip. In order to solve Maxwell's equations in the specific geometry of the tip of the tapered fiber probe and its environment, we employ the multiple multipole method (MMP) which recently has been applied to study near-field optical phenomena.[12,13] The MMP method expands the solutions on multipolar eigenfunctions. The vector multipolar eigenfunctions $\mathbf{F}_n(\mathbf{r},\omega)$ for the eigenvalue q_n satisfy the vector wave equation:

$$-\nabla\times\nabla\times\mathbf{F}_n(\mathbf{r},\omega)+q_n^2\mathbf{F}_n(\mathbf{r},\omega)=0. \tag{1}$$

In terms of scalar fields, the scalar multipolar eigenfunctions $\phi_n(\mathbf{r},\omega)$ for the eigenvalues q_n satisfy the scalar Helmholtz equation:

$$\nabla^2\phi_n(\mathbf{r},\omega)+q_n^2\phi_n(\mathbf{r},\omega)=0, \tag{2}$$

where

$$\int\phi_n^*(\mathbf{r},\omega)\phi_{n'}(\mathbf{r},\omega)dr=\delta_{n,n'} \tag{3}$$

These eigenfunctions form an orthonormal basis set in the Hilbert space. The simplest solution is obtained in Cartesian coordinates:

$$\phi_n(r,\omega)=\frac{1}{\sqrt{8\pi^3}}\exp\{j\mathbf{k}\cdot\mathbf{r}\}, \tag{4}$$

where $\mathbf{k}$ is the wave vector. The multipolar wave functions are formulated in the spherical coordinates:

$$\phi_n(r,\omega)=\phi_{\sigma,l,m,q_n}(r,\omega)=P_l^m(\cos\theta)z_l(q_nr)\begin{Bmatrix}\cos m\varphi\\ \sin m\varphi\end{Bmatrix}, \tag{5}$$

where $P_l^m(\cos\theta)$ represents for the associated Legendre polynomials and $z_l(q_nr)$ for the spherical Bessel functions. The index σ distinguishes between the even and odd functions. In the cylindrical coordinates, the multipolar wave functions are characterized as

$$\phi_n(r,\omega)=\phi_{\sigma,m,q_n}(r,\omega)=B_m(\kappa\rho)\exp\{jq_{n,z}z\}\begin{Bmatrix}\cos m\varphi\\ \sin m\varphi\end{Bmatrix}, \tag{6}$$

where the B_m are Bessel functions, $\kappa=\sqrt{q_{n,x}^2+q_{n,y}^2}$ and $\rho=\sqrt{x^2+y^2}$.

Three sets of vector eigenfunctions can be built by applying the gradient operator to the scalar functions:

$$\mathbf{L}_n(\mathbf{r},\omega) = C\nabla\phi_n(\mathbf{r},\omega), \tag{7}$$

$$\mathbf{M}_n(\mathbf{r},\omega) = C\nabla\times\phi_n(\mathbf{r},\omega)\mathbf{S}, \tag{8}$$

$$\mathbf{N}_n(\mathbf{r},\omega) = \frac{C}{k}\nabla\times\nabla\times\phi_n(\mathbf{r},\omega)\mathbf{S}, \tag{9}$$

where C is a normalization factor which relies on the coordinates system, and $\mathbf{S}$ is a constant vector of unit length, sometimes called "Poynting vector".

Because of the property of the Poynting vector and the orthonormalization of the scalar eigenfunctions, the above three sets $\mathbf{L}_n(\mathbf{r},\omega)$, $\mathbf{M}_n(\mathbf{r},\omega)$ and $\mathbf{N}_n(\mathbf{r},\omega)$ are mutually orthogonal in the Hilbert sense. The following relationship can be easily proved valid for an infinite homogeneous system:

$$\sum_n\left[\mathbf{L}_n(\mathbf{r},\omega)\cdot\mathbf{L}_n^*(\mathbf{r}',\omega)+\mathbf{M}_n(\mathbf{r},\omega)\cdot\mathbf{M}_n^*(\mathbf{r}',\omega)+\mathbf{N}_n(\mathbf{r},\omega)\cdot\mathbf{N}_n^*(\mathbf{r}',\omega)\right]=\delta(\mathbf{r}-\mathbf{r}'). \tag{10}$$

The longitudinal eigenfunctions $\mathbf{L}_n(\mathbf{r},\omega)$ have no physical meaning for our discussion. Therefore, after dividing the space in subdomains where the refractive index is constant, the MMP method performs the expansion of the electric field in each subdomain only on the sets of transverse eigenfunctions $\mathbf{M}_n(\mathbf{r},\omega)$ and $\mathbf{N}_n(\mathbf{r},\omega)$:

$$\mathbf{E}^p(\mathbf{r},\omega) = \sum_n[a_n^p\mathbf{M}_n(\mathbf{r},\omega)+b_n^p\mathbf{N}_n(\mathbf{r},\omega)]. \tag{11}$$

The unknown coefficients a_n and b_n are then determined from the electromagnetic boundary conditions on the interfaces between adjacent subdomains by a least-squares minimization.

The multipolar functions used in the basis set of the multiple multipole method are so short range that only their close neighborhood is affected. Thus the method is better suited to account for localized geometries than the expansion in plane waves.

While the electric field distribution near the tip is determined, the gradient force for a Rayleigh particle can be easily calculated as

$$\mathbf{F} = \frac{\alpha}{2}\nabla E^2, \tag{12}$$

where α is the polarizability of the particle. The particle tends to move to the higher intensity region where its induced dipole has lower potential energy. To overcome the limitation of Rayleigh approximation, a rigorous treatment of the trapping force can be performed by applying the conservation law for momentum.

The gradient force can be expressed by the Maxwell's stress tensor $\mathbf{T}$ as

$$\mathbf{F} = \int_{\partial V} <\mathbf{T}\cdot\mathbf{n}>dS, \tag{13}$$

where <...> stands for the time average, ∂V denotes a surface enclosing the particle, $\mathbf{n}$ is the outwardly directed normal unit vector, and

$$\mathbf{T} = \varepsilon_0\varepsilon\mathbf{EE}+\mu_0\mu\mathbf{HH}-\frac{1}{2}(\varepsilon_0\varepsilon E^2+\mu_0\mu H^2)\mathbf{I}. \tag{14}$$

Where, **I** stands for the unit dyad and ε, μ are the dielectric constant and magnetic permeability of the surrounding medium, respectively. For a particle in the vicinity of the tip, the magnetic contribution to the force is found approximately two orders of magnitude lower than the electric one.

The trapping potential U of a particle located at $\mathbf{r}_0$ is then given by

$$U(\mathbf{r}_0) = -\int_{\infty}^{r_0} \mathbf{F}(\mathbf{r}) \cdot d\mathbf{r} \,. \tag{15}$$

4. RESULTS AND DISCUSSIONS

The following parameters of the single-mode fiber are chosen in our calculation. The refractive indices of the core and cladding are n_1=1.4544 and n_2=1.45, respectively. The diameters of the core and cladding are respectively $2a$=8μm and $2b$=125μm. The wavelength of the illuminating light is λ=632.8nm (He-Ne laser). The fiber taper is assumed to be linear with an 100nm-tip size.

Figure 2 shows the contours of the near field distribution in the vicinity of the tip of the fiber probe with a conical taper. The near field close to the tip is mainly of evanescent components which are mostly concentrated at the axial direction. The field is rotationally symmetric in the vicinity of the tip, and attenuate rapidly with distance from the tip. So a three dimensional gradient optical field is formed near the tip of the tapered fiber probe. The field is rotationally symmetric in the vicinity of the tip since the fiber probe has a rotationally symmetric geometry.

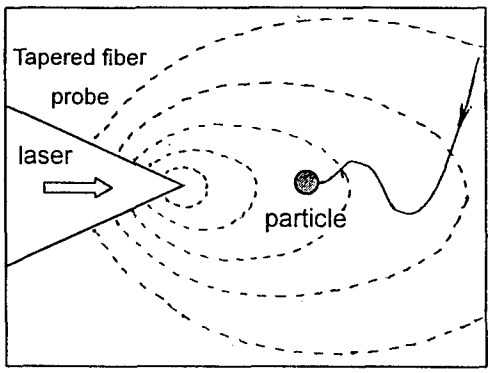

Fig.2. Contours of the near field of tapered fiber probe. The single-mode fiber is specified as n_1=1.4544, n_2=1.45, $2a$=8μm, and $2b$=125μm. The illuminating wavelength is λ=632.8nm (He-Ne laser). When a particle approaches the vicinity of the fiber tip, it will be trapped by the gradient force of the near field of the fiber probe.

Figures 3 and 4 give the intensity distributions of the near fields out of the tip as functions of the longitudinal and transverse distances (z and x, respectively) from the tip, respectively. Since the optical near field in the vicinity of the tip is evanescent, the field amplitude reduces dramatically with the distance from the tip, and shows almost rotationally symmetric in the vicinity of the tip.

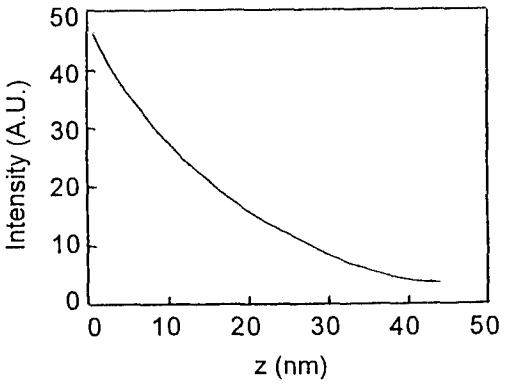

Fig.3. Intensity distribution of the near field of the tip along the longitudinal direction z. The illuminating wavelength is λ =632.8nm (He-Ne laser). The tip diameter of the fiber probe is assumed as 100nm.

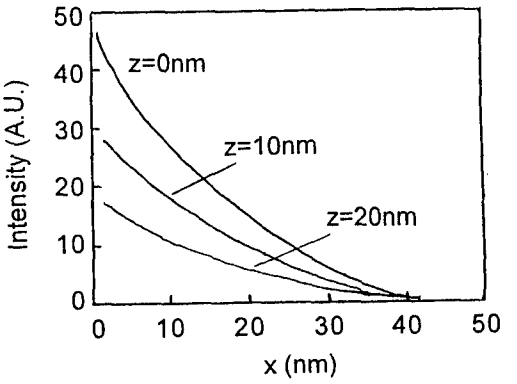

Fig.4. Intensity distribution of the near field of the tip along the transverse direction x with different longitudinal distances (z=0, 10nm and 20nm, respectively). The field is rotationally symmetric in the vicinity of the tip.

In our calculation, the interaction of the tip and a nanometric particle close to the tip is not counted. However, the field distributions will be distorted around a dielectric particle. A rigorous treatment of the gradient field and the trapping force may be performed by applying the conservation law for momentum.[14]

When a particle (of diameter d=10nm) approaches the fiber tip, the trapping force and the potential energy can be calculated from the above equations (12) to (15). Figures 5 and 6 show cross sections of the trapping potential along the axial (z) and lateral (x) directions from the tip, respectively. Since the trapping potential is almost rotationally symmetric, we only show the results for the (x, z) plane.

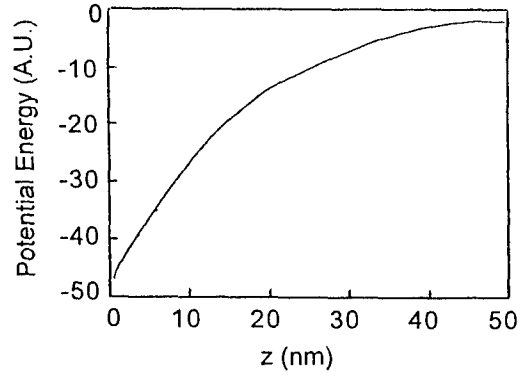

Fig.5. Normalized trapping potential energy of a particle (of diameter d=10nm) as the function of the longitudinal distance z from the tip.

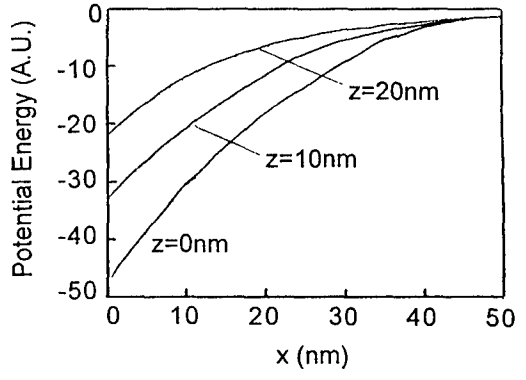

Fig.6. Normalized trapping potential energy of a particle (d=10nm) as the function of the transverse distance x from the tip, with different longitudinal distances (z=0, 10nm and 20nm, respectively).

The trapping potential is sensitively dependent upon the size, shape and dielectric constant of the trapping particle, as well as the size and refractive index of the fiber tip. Generally, the trapping force is inversely proportional to the tip size, and a sharper tip is required for trapping smaller particles.

The trap force may be affected by the wavelength of the incident light. The particle can be trapped and approach the probe for one wavelength, however, it is also possible to be repelled and escape from the probe for another wavelength. By the wavelength-dependent optical force, one can trap, move, and deposit the particle on a desired position on a nanometer scale.

5. CONCLUSIONS

A method performing near-field optical trapping by a tapered fiber probe has been presented in this paper. Since the fiber probe has a nanometer-scaled resolution, the near-field optical trap is better suited to trap smaller particles. The multiple multipole method is employed to calculate the near field in the vicinity of the fiber tip and obtain the trapping force for a dielectric particle. The calculation results indicate the feasibility of the method.

Compared with the optical trap by a highly focused laser beam, the near-field optical trap using a tapered fiber probe exhibits the following advantages: (1) the optical trapping system is simplified without focusing objective lenses; (2) the fiber is conveniently coupled with a laser diode acted as the illuminating source, so that high a coupling efficiency is easily obtained; (3) the highly confined evanescent fields significantly reduce the trapping volume; (4) the large field gradients result in a large trapping force; and (5) the trapped particles can be moved precisely and freely when the fiber probe is mounted on the three dimensional scanning set-up of the SNOM system.

The experiment of the near-field optical trapping is in progress, and the experimental results will be reported in another article in the near future.

ACKNOWLEDGMENTS

We are very grateful to Prof. Hai Ming and Dr. Ming Bai of University of Science and Technology of China for many helpful discussions. This research is supported financially by Central China Normal University.

REFERENCES

1. Ashkin, J. M. Dziedzic, J. E. Bjorkholm and S. Chu, "Observation of a single-beam gradient force optical trap for dielectric particles," *Opt. Lett.*, 1986, **11**, pp.288-290
2. W. H. Wright, G. J. Sonek, Y. Tadir and M. W. Berns, "Laser trapping in cell biology," *IEEE J. Quantum Electron.*, 1990, **26**, pp.2148-2157
3. K. Taguchi, H. Ueno, T. Hiramatsu and M. Ikeda, "Optical trapping of dielectric particle and biological cell using optical fibre," *Elect. Lett.*, 1997, **33**(5), pp.413-414
4. Zhang Guoping, Ming Hai, Chen Xiaogang, Yang Bao, Xie Jianping, "Experiment Researches on Active Fiber Probe for Scanning Near-field Optical Microscopy," *Chinese J. of Lasers*, 1997, **B6**, pp.513-517
5. E. Betzig, and J. K. Trautman, "Near-field optics: microscopy, spectroscopy, and surface modification beyond the

diffraction limit," *Science*, 1992, **257**, pp.189-195

6. H. Heinzelmann, and D. W. Pohl, "Scanning near-field optical microscopy," *Appl. Phys. A*, 1994, **59**, pp.89-101
7. W. Jhe, "Photon scanning tunneling microscope and optical nanotechnology," *AAPPS Bulletin*, 1995, **5**(1&2), pp.12-14
8. Zhang Guoping, Ming Hai, Chen Xiaogang, Wu Yunxia, Xie Jianping, "Transmission properties of two kinds of fiber probes in scanning near-field optical microscope," *Acta Optica Sinica*, 1998, **18**(7), pp.886-889
9. Zhang Guoping, Ming Hai, Chen Xiaogang, Wu Yunxia, Xie Jianping, "Effect of the Taper Shape upon Transmission Efficiency of Fiber Probes for Scanning Near-field Optical Microscopy," *Chinese J. of Lasers*, 1998, **B7**, pp.357-362
10. G. A. Valaskovic, M. Holton and G. H. Morrison, "Parameter control, characterization, and optimization in the fabrication of optical fiber near-field probes," *Appl. Opt.*, 1995, **34**, pp.1215-1228
11. Zhang Guoping, Ming Hai, Chen Xiaogang, Yang Bao, Xie Jianping, "Research and development of active fiber probe for scanning near-field optical microscope," *Semiconductor Optoelectronics*, 1997, **18**, pp.250-252
12. Ch. Hafner, *The Generalized Multiple Multipole Technique for Computational Electromagnetics*, Artech, Boston, 1990
13. Lukas Novotny, Randy X. Bian and X. Sunney Xie, "Theory of nanometric optical tweezers," *Physical Review Letters*, 1997, **79**(4), pp.645-648
14. J. A. Stratton, *Electromagnetic Theory*, McGraw_Hill, New York, 1941